ceramics

MDPI

Article

Valorization of Industrial Waste in Monoporosa Ceramic Tile Production

Caterina Sgarlata [1,*], Luciana Cupertino [1], Lorenzo Serafini [2] and Cristina Siligardi [1,*]

[1] Department of Engineering "Enzo Ferrari", University of Modena and Reggio Emilia, Via Pietro Vivarelli 10, 41125 Modena, MO, Italy
[2] Gruppo Concorde S.p.A., Via del Canaletto, 77, 41042 Fiorano Modenese, MO, Italy; l.serafini@gruppoconcorde.it
* Correspondence: caterina.sgarlata@unimore.it (C.S.); cristina.siligardi@unimore.it (C.S.)

Abstract

The ceramics industry has long embraced the principles of the circular economy, with a strong focus on the reuse and recovery of raw materials essential to the production cycle. This approach reduces costs by reintroducing secondary raw materials—such as production scraps and recycled materials—into the manufacturing process after appropriate recovery treatments. This study aims to contribute to the transition of the ceramic industry toward a circular economy by incorporating industrial by-products into monoporosa ceramic bodies, thereby transforming waste materials into valuable resources. Monoporosa is a porous, single-fired ceramic wall tile characterized by a high carbonate content and low bulk density. However, the role of secondary raw materials in monoporosa formulations, as well as their influence on processing behavior (e.g., during sintering) and on key technological properties, is not yet fully understood. This work investigates a standard monoporosa formulation based on conventional raw materials (sand, calcite, feldspars, and clays) and compares it with new formulations in which industrial waste materials from local and national sources—originating from other industrial processes—are used as partial or total substitutes for some of the traditional raw materials, particularly sand and calcite. The industrial by-products examined include biomass bottom ash, foundry sand, and marble cutting and processing sludge. All materials were characterized using chemical–mineralogical, thermal, and morphological analyses and were incorporated into the ceramic bodies at different substitution levels (10%, 50%, and 100%) to replace natural raw materials. Their behavior within the mixtures was evaluated to determine ceramic suitability and acceptable replacement ratios. Furthermore, the effects of these additions on water absorption, thermal expansion coefficient, and microstructural characteristics were assessed. Based on the positive results obtained, this study demonstrates the feasibility of using, in particular, two secondary raw materials—foundry sand and marble sludge—in monoporosa body formulations, allowing for the complete replacement of the original raw materials and thereby contributing to the development of more sustainable ceramic compositions.

Keywords: monoporosa; industrial by-products; foundry sands; bottom ash; marble waste

Academic Editors: Gilbert Fantozzi and Vincent Garnier

Received: 5 November 2025
Revised: 23 January 2026
Accepted: 27 January 2026
Published: 28 January 2026

1. Introduction

Ceramic tiles produced by pressing are among the most widely used materials in the construction and interior design sectors. This is due to their versatility, durability, and

ability to combine aesthetics with functionality [1–3]. Among the various types of ceramic tiles, porcelain stoneware, monoporosa, single-fired, double-fired, and third-firing tiles can be identified [4,5]. With the advent of advanced forming and decoration technologies, the latter three types have almost disappeared from the Italian industrial landscape. Porcelain stoneware has become the leading and most widely produced ceramic product—at least in Italy—while monoporosa remains a niche product due to its specific characteristics [6]. Porcelain stoneware has emerged as the most widespread and commercially successful ceramic product worldwide. It is a compact, non-porous ceramic material primarily composed of sand, feldspar, plastic clays, and kaolin. It is produced through grinding, spray-drying, pressing, decoration, and firing at high temperatures. This manufacturing process imparts exceptional properties, including high resistance to wear, impact, and chemical attack. It also results in very low water absorption, making the material suitable for wet environments such as bathrooms and kitchens [7,8]. In addition, its aesthetic versatility allows it to replicate the appearance of natural materials such as marble, wood, or stone. As a result, porcelain stoneware is used in a wide range of applications, both residential and commercial. These include flooring, wall cladding, interior and exterior spaces, and high-traffic environments such as airports and shopping centers [3,9]. Monoporosa, by contrast, is a porous, single-fired ceramic wall tile characterized by a high carbonate content and produced through a manufacturing process similar to that of porcelain stoneware. The main difference lies in the mineralogical composition of the ceramic body, which contains a significant proportion of carbonates [10]. These single-fired wall tiles represent an ideal solution for interior wall coverings due to their lightweight and porous ceramic body. This structure ensures easy handling, rapid installation, and good adhesion. Finished with smooth, glossy glazes, monoporosa tiles offer a wide range of aesthetic possibilities. At the same time, they maintain uniform surface quality and dimensional regularity. They are particularly suitable for bathrooms, kitchens, and residential or light commercial interiors. In these applications, they provide an effective balance between aesthetics, functionality, and cost efficiency [11–13]. Over the years, extensive research has focused on improving the understanding of monoporosa materials. This has been achieved through both fundamental and applied studies [6,14,15]. Additional efforts have been devoted to optimizing ceramic body formulations for this application [13,16]. A key aspect of the modern ceramic industry is its increasing focus on sustainability. In this context, the use of secondary raw materials plays a crucial role. These materials, derived from industrial and ceramic waste recycling processes, are integrated into production cycles to reduce environmental impact. Their use contributes to limiting the extraction of natural resources and reducing waste generation. It also promotes circular economy principles and lowers CO_2 emissions by decreasing energy consumption during production. In recent years, numerous studies have investigated the use of secondary raw materials in ceramic applications. These studies have focused particularly in porcelain stoneware [17–20], ceramic bricks [21,22], and other ceramic materials [23,24]. However, despite the extensive literature on porcelain stoneware, monoporosa single-fired tiles have received considerably less attention. This is especially true for innovative formulations incorporating waste materials. Only a limited number of studies are currently available [11,14]. Consequently, knowledge regarding the role of waste materials in monoporosa formulations remains scarce. Their influence on processing behavior, such as during sintering, and on key technological properties is still not fully understood. This study presents research on a standard monoporosa formulation based on traditional raw materials. These include sand, calcite, feldspars, and clays. The study also investigates new formulations incorporating industrial waste materials from local and national sources. These materials originate from

other industrial processes. They are used as substitutes for conventional raw materials, particularly sand and calcite. The waste materials considered in this study are:

1. Bottom ash from biomass plant;
2. Foundry sand;
3. Cutting and processing dust from marble.

Numerous technologies have been developed for the thermochemical conversion of biomass, particularly for combustion processes. However, all biomass combustion systems inherently generate a considerable quantity of solid residues. The ash content typically ranging from 5% to 15% by weight of the processed biomass [25]. These residues are primarily the result of thermal degradation mechanisms such as combustion, pyrolysis, and incineration of lignocellulosic feedstocks. The ash produced is generally classified into two main categories: bottom ash and fly ash. The physicochemical characteristics of these ashes can vary significantly. This variability depends on the biomass feedstock, combustion parameters, and the specific technology employed. Elevated ash content adversely affects the energy yield of biomass, reducing the overall efficiency of the conversion process [26]. Moreover, as the global demand for bioenergy continues to rise, the generation of ash and other combustion residues is expected to increase proportionally. This trend poses additional challenges for sustainable waste management and resource recovery.

About foundry sand, across Europe, an estimated 3000 foundries are currently in operation, collectively producing more than 11 million tonnes of waste foundry sand each year. Ferrous metal foundries account for the majority of this waste stream. At present, only approximately 25% of this waste sand is subject to recovery or reuse. This typically in limited applications such as cement manufacturing. However, these end-use markets are insufficient to accommodate the total volume of material generated. Consequently, around 75% of the spent foundry sand is disposed of. Disposal mainly occurs through landfilling or low-value applications such as use in road base layers. Italy ranks as the second-largest foundry producer in Europe and ninth globally in terms of output. Approximately 80% of Italian foundries are concentrated in the northern regions of the country [27]. Several studies have been conducted to evaluate the potential reuse of waste foundry sands derived from cast iron production as a secondary raw material in the manufacturing of construction materials. These materials include products obtained through high-temperature processes as well as those consolidated at room temperature [28–30]. However, the production of dimension stones generates significant quantities of extractive waste. This waste represents a major source of environmental concern (materials removed during extraction activities, topsoil, overburden, residues produced during the processing of industrial minerals) [31]. At the European level, extractive waste is the second largest source of waste generation. It accounts for approximately 622 million tons per year, which corresponds to 26.6% of the EU's total waste production [32].

All the materials used will be characterized through chemical-mineralogical analysis (XRF, XRD, laser granulometry), thermal analysis (TG-DTA), and morphological analysis using scanning electron microscopy (SEM-EDS). The SRMs will be incorporated into the mixtures at different replacement levels (10%, 50%, and 100%). The mixtures will be evaluated for ceramic suitability and optimal substitution rates. The resulting formulations will be characterized by granulometry, XRD, apparent density, water absorption, linear shrinkage, SEM/EDS, and thermal expansion to assess their effects on physical and morphological properties.

2. Materials and Methods

2.1. Monoporosa Standard Preparation

Monoporosa is a ceramic material primarily used for the production of outdoor tiles. Its commercial success is due to its excellent properties, which make it suitable for various types of cladding. For the production of monoporosa samples, the following raw materials were used:

- Clay;
- Sand;
- Calcite;
- Chamotte from Gruppo Concorde (waste).

The raw materials were supplied by Gruppo Concorde, and the standard formulation is shown in Table 1. Chemical analysis of the raw materials is reported in Table 2.

Table 1. Mix of monoporosa standard.

Raw Materials	Percentage (wt%)
sand	26
clay	44
calcite	10.5
chamotte	19.5

Table 2. Chemical analysis of the raw materials of the standard composition.

Raw Material	SiO_2	Al_2O_3	Fe_2O_3	TiO_2	CaO	MgO	Na_2O	P_2O_5	K_2O	Cr_2O_3	Ther Oxides	PF (%)
clay	60.8	22.128	3.211	0.902	0.983	0.53	0.19	0.055	2.505	0.013	0.108	7.91
sand	81.91	8.091	0.632	0.107	1.989	0.272	1.427	0.017	3.141	/	0.067	1.92
calcite	3.38	0.77	0.31	0.01	51.8	0.96	<0.01	/	0.06	/		42.5
chamotte	72.015	17.97	0.93	0.579	1.4	0.527	3.558	0.203	2.249	0.082	0.366	0.15

To prepare the mixtures, the raw materials were first dried and sieved using a 2 mm mesh. Water (270 g) and sodium tripolyphosphate ($Na_5P_3O_{10}$), used as a deflocculant (0.5 wt.% of the mixture), were added to 500 g of the raw materials. The slip was obtained by mixing the components in a porcelain jar with an equivalent mass of 18 mm diameter alumina balls, which facilitated homogenization. The mixture was then milled in a rotating mill at 500 rpm for 15 min. The resulting slip was poured into an aluminum tray through a 1 mm sieve to ensure a particle size distribution with a D90 below approximately 40 µm. The slip was subsequently dried in an oven at approximately 100 °C until complete dehydration. The dried material was crushed using a mortar, sieved again through a 1 mm mesh, and moistened with 6 wt.% water (dry basis). The humidified mixture was then shaped by uniaxial pressing using a hydraulic press (Nannetti, Faenza, RA; Italy) at 22 bar (300 kg/cm^2). Finally, the dried samples (80 °C for 24 h) were fired in an industrial kiln (Gruppo Concorde, Fiorano Modenese, Mo, Italy) at a maximum temperature of approximately 1160 °C, with a total firing cycle of 45–50 min.

2.2. Monoporosa New Formulations

The new mixtures were formulated by replacing specific percentages of sand or calcite in the standard monoporosa composition with secondary raw materials (SRMs). Table 3 reports the compositions of the newly developed formulations. In these mixtures, SRMs were used as substitutes for either sand or carbonates at different replacement levels in

order to evaluate their effects on the chemical–physical, mineralogical, mechanical, and microstructural properties of the ceramic bodies. The replacement levels investigated were 10%, 50%, and 100%. In each formulation, only one raw material was replaced at a time—either sand or calcite—while all other raw materials remained unchanged with respect to the standard mixture. The specific replacement percentages for each formulation are detailed in Table 3.

Table 3. Compositions of the new formulations with the SRMs.

Sample	Clay (%)	Sand (%)	Calcite (%)	Chamotte (%)	Bottom Ash (%)	Foundry Sand (%)	Carrara Marble (%)
BA 10	44	23.4	10.5	19.5	2.6	/	/
BA 50	44	13	10.5	19.5	13	/	/
BA 100	44	0	10.5	19.5	26	/	/
FS 10	44	23.4	10.5	19.5	/	2.6	/
FS 50	44	13	10.5	19.5	/	13	/
FS 100	44	0	10.5	19.5	/	26	/
CM 10	44	26	9.45	19.5	/	/	1.05
CM 50	44	26	5.25	19.5	/	/	5.25
CM 100	44	26	0	19.5	/	/	10.5

The SRMs used as substitutes for sand were:

- Biomass Bottom ash;
- Foundry sand.

The SRM used as a substitute for calcite was:

- Marble processing sludge

The percentage of SRM replacing sand was always calculated with reference to the 26% sand content in the standard formulation. Similarly, for formulations where calcite was replaced, the calculations were always based on the total calcite percentage (10%, 50%, 100% by weight). All other SRMs were incorporated into the mixture as complete (100%) substitutes for the base raw material (either sand or carbonates). The new mixtures were prepared following the same procedure as the standard monoporosa mixture described earlier. The firing process was also carried out using the same industrial kiln cycle, with a maximum temperature of 1160 °C and a total firing duration of 45–50 min.

2.3. Materials Characterization

The particle size distribution of the raw materials and secondary raw materials (SRMs) was determined using a Malvern Mastersizer 2000 laser granulometer equipped with a Hydro 2000S module (Malvern Worcestershire, UK), employing 1 g of powder dispersed in water. Thermogravimetric analysis (TGA) and differential scanning calorimetry (DSC) were performed using a Netzsch STA 429 instrument (NETZSCH-Gerätebau GmbH, Selb, Germany) in the temperature range of 25–1400 °C at a heating rate of 10 °C·min^{-1} to evaluate the thermal transformation reactions of the mixtures. The microstructural properties of the investigated materials were further analyzed by scanning electron microscopy (SEM; Quanta 200, FEI–Thermo Fisher Scientific, Eindhoven, The Netherlands) coupled with an energy-dispersive X-ray (EDX) detector (INCA, Oxford Instruments Analytical, Oxford, UK) for qualitative and semi-quantitative chemical analysis. SEM micrographs and EDX spectra were acquired using an electron beam energy of 25 keV. Prior to analysis, the

samples were sputter-coated with a thin gold (Au) layer to ensure electrical conductivity. Qualitative mineralogical analysis was carried out by powder X-ray diffraction (XRD) using a PW3710 diffractometer (Philips, Almelo, The Netherlands) with Cu-Kα radiation (λ = 1.54 Å) generated by a conventional X-ray source operating at 35 kV and 35 mA, with a step size of 0.008°. Both powdered samples and the surfaces of fired specimens were scanned over an angular range of 5–70° (2θ), and the diffraction patterns were analyzed using PANalytical HighScore Plus software (version 5.1). An optical dilatometer (Expert System) was employed to determine the sintering temperatures of the unfired monoporosa formulations, previously dried at 105 °C for 12 h, using bar-shaped specimens with dimensions of 1.5 cm × 0.5 cm. A controlled heating rate of 20 °C·min^{-1} was applied up to the melting temperature. Linear shrinkage (LS, %) of fired discs at different temperatures was determined using a precision caliper by measuring the diameter of the fired specimens and comparing it with the diameter of the press cavity (50 mm), according to the equation $LS\ (\%) = (L_2 - L_1)/L_2$, where L_2 is the diameter of the press cavity and L_1 is the diameter of the fired sample. Water absorption (WA, %) was measured using a deprimometer by placing the discs on a sieve and applying a vacuum of 0.1 bar for 30 min, followed by water introduction to fully immerse the specimens for an additional 15 min. The samples were then removed, surface-dried, and weighed using a precision balance with an accuracy of four decimal places. The color of the fired samples was evaluated using a PCE-CSM colorimeter and expressed in the CIE Lab* color space, where Lrepresents lightness (0 = black, 100 = white), a corresponds to the green–red axis, and b to the blue–yellow axis (accuracy ±0.1). Color differences were quantified by calculating the total color difference (ΔE), which represents the perceptible difference in color between each sample and the reference standard in the CIE Lab color space.

3. Results

3.1. Monoporosa Standard

The particle size distribution of the mixture is shown in Figure 1. The distribution is relatively broad, with characteristic diameters of D10 ≈ 1.35 µm, D50 = 7.21 µm, and D90 = 34.23 µm. This distribution reflects the heterogeneous nature of the mixture. The mixture includes raw materials such as clays, sand, limestone, and industrial waste. All these components fall within the same granulometric range. In granulometric analyses, particular attention is typically paid to the D90 value, defined as the particle diameter below which 90% of the particles are contained. From an industrial perspective, the required granulometric range is generally between 34 µm and 42 µm. Therefore, the obtained results fully comply with industrial specifications.

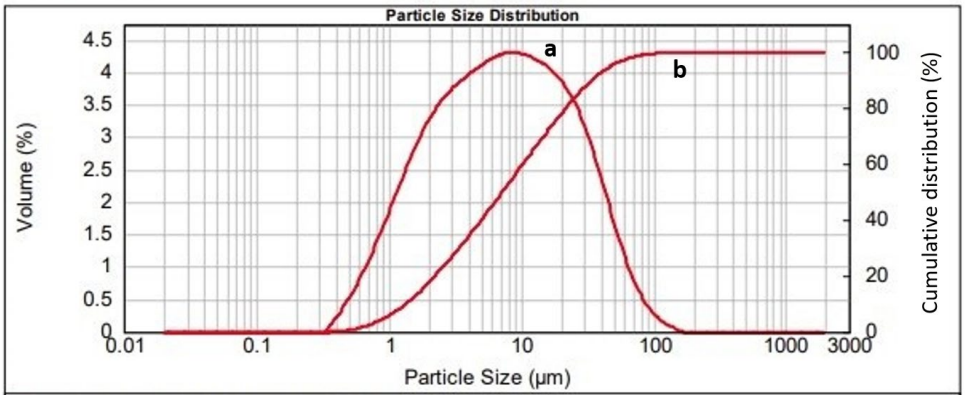

Figure 1. Particle volume distribution (a) and cumulative distribution (b) curves of monoporosa STD mixture.

Figure 2 shows the XRD patterns of the fired mixture. This pattern highlights the mineralogical nature of the monoporosa body after firing. The crystalline phases reported are quartz (ref.code 01-079-1910), albite calcian (ref.code 01-079-0927), and anorthite (ref.code 00-009-0478). These phases are predominantly neoformations (plagioclases) that result from solid-state reactions between clays and carbonates, and from the sand, which acts as the inert component of the mixture. Additionally, a vitreous phase is present. Its content is in not high and is generally around 20–30%, as reported in the literature [33].

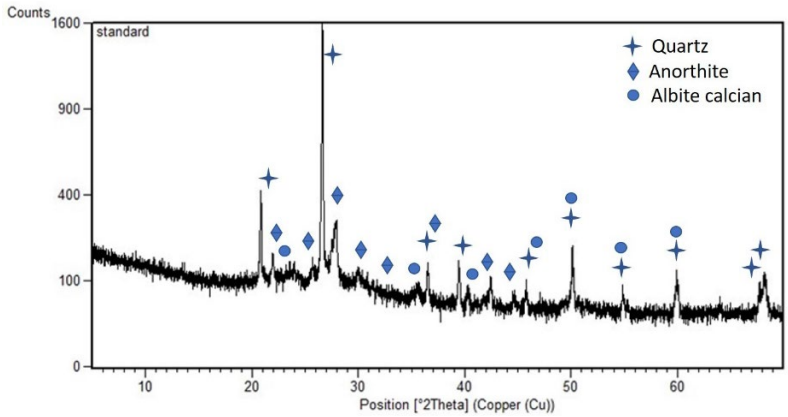

Figure 2. XRD patterns of the fired Standard formulation with the crystalline phases.

The thermogravimetric analysis shown in Figure 3 highlights the mass variations occurring in the mixture during thermal treatment. The mass loss observed in the temperature range of approximately 400–500 °C is associated with the thermal reactivity of the clay minerals. The mass loss starting at around 700–800 °C is attributed to the decomposition of the carbonates present in the mixture. During firing, these carbonates decompose, releasing CO_2. The DSC curve also exhibits peaks corresponding to the aforementioned events. The other peaks are associated with the α-quartz to β-quartz phase transformation at 571 °C and the melting of some crystalline phases at approximately 1181 °C.

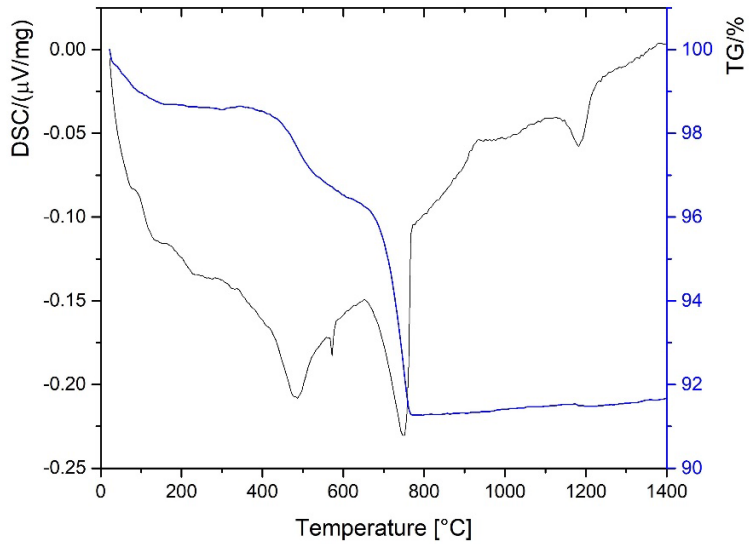

Figure 3. Standard formulation thermogravimetric analysis.

The optical dilatometry thermogram (Figure 4) highlights a slight contraction after the decomposition of the clays. It also shows a continuous expansion up to 950 °C due to the decomposition of carbonates. Subsequently, the sintering process reaches its peak at approximately 1050 °C. At higher temperatures, a slight expansion is observed.

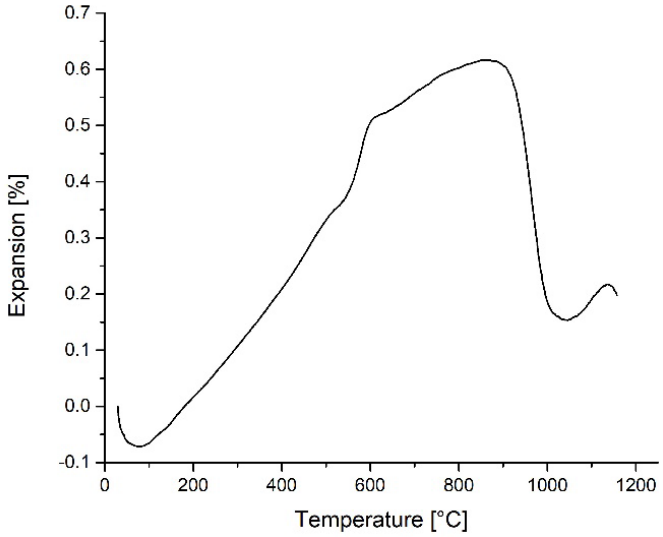

Figure 4. Standard formulation optical dilatometry thermogram.

The images presented below correspond to scanning electron microscopy (SEM) micrographs of the fired materials. Figure 5 shows the standard sample observed at a magnification of 1000×. A semi-quantitative energy-dispersive X-ray spectroscopy (EDS) analysis was also performed to evaluate the relative abundance of selected elements in specific areas of the specimen. Figure 5 includes the EDS results, expressed as oxide percentages (i.e., elements bonded to oxygen), obtained from a selected area of the sample. Multiple spectra were acquired at different points within the analyzed area to determine the average chemical composition of the specimen. The magnified micrograph reveals a porous microstructure. Some crystalline phases are inherited from the raw materials and others formed as neoformed phases during firing. This observation is as also confirmed by X-ray diffraction analysis.

The technological properties of the standard mixture, including apparent density, linear shrinkage, and water absorption, were evaluated. The results are summarized in Table 4. They are reported as the average of three measurements. All values fall within the typical industrial ranges for monoporosa tiles. These tiles are characterized by high water absorption due to their elevated porosity and low linear shrinkage as a result of incomplete sintering. Sintering occurs at firing temperatures lower than those commonly employed for porcelain stoneware.

Table 4. Water absorption (WA), Linear shrinkage (LS), Apparent density (AD) of monoporosa STD.

Monoporosa Standard	Values
WA (%)	17.63 ± 0.13
LS (%)	0.3 ± 0.02
AD (g/cm^3)	1.78 ± 0.002

3.2. Characterization of Secondary Raw Materials

Before replacing the selected raw materials in the standard mixture, a characterization process was carried out to assess their suitability. The secondary raw materials used are as follows:

- Marble processing sludge;
- Bottom ash;
- Foundry sand.

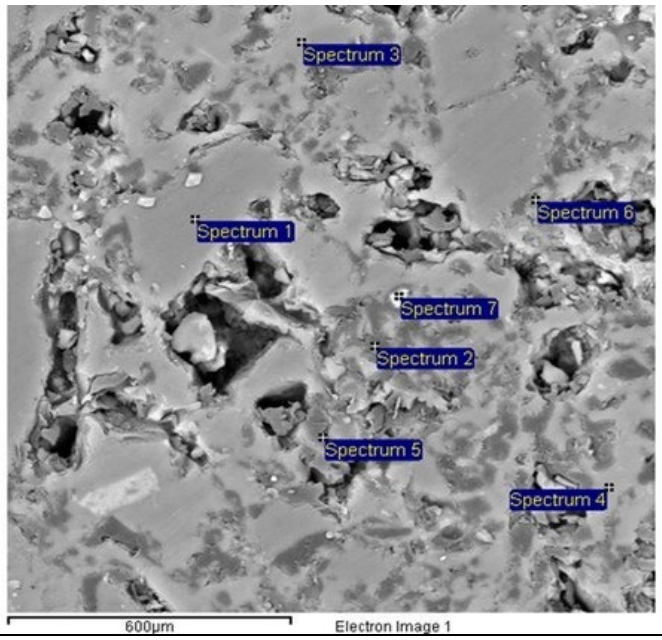

Sprectrum Label	Na	Mg	Al	Si	K	Ca	Ti	Fe	Total
Spectrum 1	0.09	0.00	0.25	99.35	-	0.12	-	0.19	100
Spectrum 2	1.76	1.20	19.57	58.16	6.99	10.43	0.41	1.49	100
Spectrum 3	1.43	0.52	13.78	73.50	1.75	7.21	0.29	1.52	100
Spectrum 4	1.12	0.68	19.15	61.39	2.40	11.80	1.22	2.25	100
Spectrum 5	0.62	0.56	6.10	88.22	1.54	1.77	0.30	0.90	100
Spectrum 6	2.71	0.85	20.43	63.62	6.48	4.70	0.35	0.86	100
Spectrum 7	0.73	0.69	3.69	11.51	0.58	0.92	1.09	80.79	100

Figure 5. Standard sample observed at a magnification of 1000× with EDS analysis.

All secondary raw materials were characterized to determine their chemical, physical, and mineralogical properties. The corresponding results are presented in this section. One of the characterized materials is a sludge derived from marble cutting and processing. This process generates a white sludge, which was considered as a potential substitute for calcium carbonate in the ceramic body formulation. In Italy, bottom ashes are classified as non-hazardous waste. They are currently used only to a limited extent as raw materials in the cement industry and are already employed in other sectors related to building material production. For this reason, this material was characterized to evaluate its potential applicability as a secondary raw material in the ceramic tile industry. Spent foundry sand is a by-product of the metal casting industry. It originates from both ferrous and non-ferrous processes. Foundry sands may contain more than 80 wt.% SiO_2, along with minor amounts of iron oxides derived from the casting process. Their physical and mechanical properties depend primarily on mineralogical composition, particle morphology, and granulometric distribution. Foundry sands are classified as non-hazardous waste and can be reused in other industrial sectors as secondary raw materials; for example, they have been applied in sustainable construction, particularly in cold-formed materials such as cementitious composites, asphalt mixtures, concrete, and cement. Owing to their high silica content, foundry sands are of particular interest as potential substitutes for the inert sands commonly used in ceramic tile production. The chemical compositions of the investigated secondary raw materials are reported in Table 5. X-ray fluorescence (XRF) analysis revealed that marble is predominantly composed of CaO, with all other elements present at concentrations below 1 wt.%.

Table 5. XRF analysis bottom ash and foundry sand.

	Bottom Ash		Foundry Sand		Carrara Marble
Oxides	**wt (%)**	**Element (ppm)**	**wt (%)**	**Element (wt%)**	**wt (%)**
SiO_2	58.98	S (366)	93.00	C (0.18)	0.5
Al_2O_3	11.30	Cr (121)	2.03	S (0.05)	0.1
K_2O	8.59	F (136)	0.71		/
CaO	9.56	Cl (98)	0.12		54.20
MgO	3.49		0.16		1.20
Fe_2O_3	5.16		1.48		0.01
Na_2O	1.09		/		/
TiO_2	0.75		0.37		/
P_2O_5	0.90		/		/
ZrO_2	/		1.89		/
LOI	/		0.24		54.20
Others	0.18		/		/

Examination of the chemical composition of the bottom ash indicates that the main oxides detected are those typically found in ceramic formulations, such as SiO_2, Al_2O_3, CaO, MgO, and Fe_2O_3. However, iron oxide is present in relatively high concentrations, which could influence the coloration of the ceramic body. Nevertheless, because monoporosa tiles are wall tiles, color is generally less critical than in other ceramic products, such as porcelain stoneware. X-ray fluorescence (XRF) analysis of the foundry sand shows a very high SiO_2 content (approximately 93 wt.%), together with a certain amount of iron oxide. It should be noted that the sand did not undergo any deferrization treatment; therefore, its iron content could be further reduced, if necessary, by magnetic separation, which is a common practice in ceramic production. The mineralogical characterization of the secondary raw materials is reported in Figure 6. The figure presents the diffraction patterns and the corresponding identified crystalline phases. The XRD analysis of marble sludge reveals calcite as the sole mineralogical phase, with diffraction peaks in Figure 6a corresponding to $CaCO_3$. The X-ray diffraction pattern of the bottom ash (Figure 6b) indicates the presence of a glassy phase. It also reveals crystalline phases such as quartz and a potassium aluminosilicate. The XRD analysis of the foundry sand (Figure 6c) shows quartz (SiO_2) as the predominant phase. Potassium feldspar ($KAlSi_3O_8$) and zircon ($ZrSiO_4$) are also present as secondary phases but technologically relevant phases for mold production. In particular, zircon helps limit oxygen reactivity with molten metal. Minor amounts of clay, used as a binder in foundry applications, may also be present but are not detectable in the diffractogram.

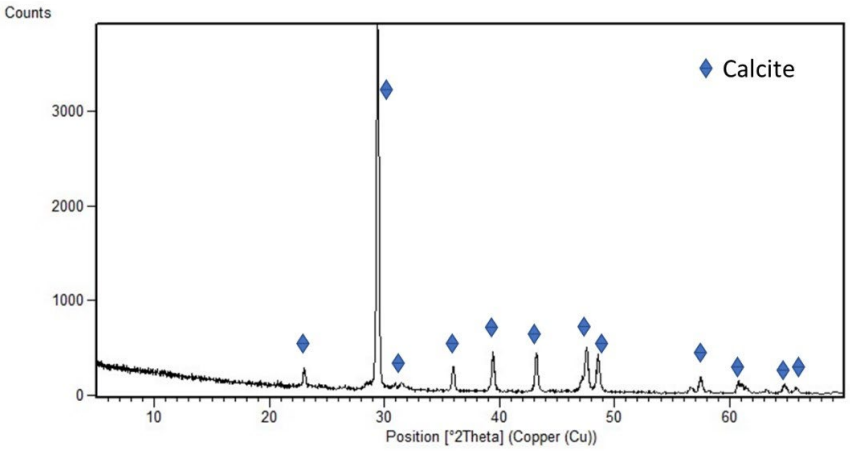

(**a**) Carrara marble

Figure 6. *Cont.*

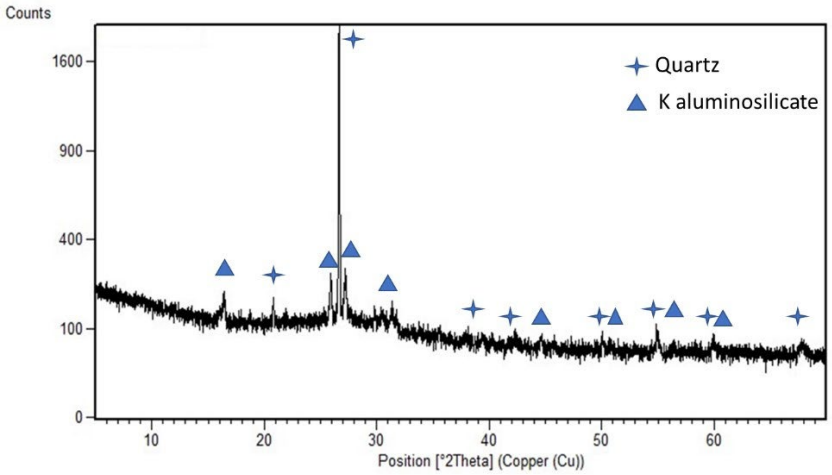

(**b**) Bottom ash

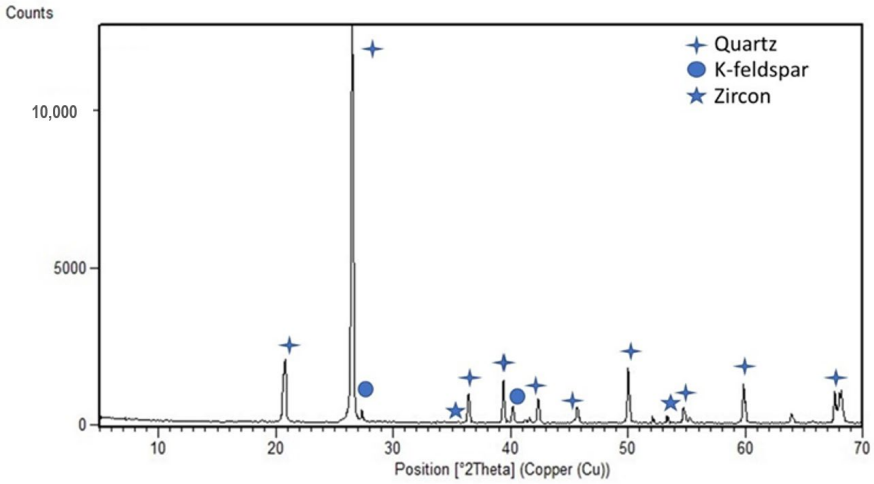

(**c**) Foundry sand

Figure 6. XRD analysis of the carrara marble (**a**), the bottom ash (**b**) and the foundry sand (**c**) with the crystalline phases.

The thermogram of the TG/DSC analysis of marble sludge in Figure 7 shows a significant weight loss in the TG curve at 829 °C, along with the corresponding endothermic event in the DSC curve. This is due to the thermal decomposition of calcium carbonate ($CaCO_3$), which typically occurs between 800 and 900 °C.

The thermal decomposition reaction of calcium carbonate is as follows:

$$CaCO_3 \rightarrow CaO + CO_2$$

This result is particularly interesting because the marble from Carrara marble processing proves to be suitable for replacing calcite in the monoporosa ceramic mixture.

A TG–DSC analysis was also performed on the bottom ash powder to evaluate its behavior under thermal treatment from room temperature to high temperatures. The thermogram shown in Figure 7 highlights the mass variations and the thermal reactivity of the phases present in the raw powder. The thermogravimetric curve indicates an overall mass loss of approximately 2 wt.%. This mass loss is mainly attributable to moisture release (>1 wt.% around 100 °C) and to the presence of volatile compounds in the temperature range of approximately 400–600 °C. Beyond this range, the sample remains relatively stable up to the typical firing temperature of monoporosa bodies (≈1150 °C). The DSC

curve reveals crystallization exothermic peaks at 849 °C and 957 °C. An endothermic peak is associated with a melting phenomenon at approximately 1188 °C. Table 6 reports the particle size distribution of the secondary raw materials (SRMs), expressed as D10, D50, and D90 values. A clear difference in granulometry among the three waste materials can be observed. Carrara marble exhibits a very fine particle size distribution, with a D50 of approximately 10 μm. Foundry sand follows, with a D50 of approximately 100 μm, and bottom ash with a coarser distribution, characterized by a D50 of approximately 192 μm. The particle size distribution of the foundry sand is very similar to that of sands commonly employed in the ceramic industry. These results confirm that foundry sand is suitable for replacing conventional sands used in ceramic tile production, particularly in monoporosa formulations.

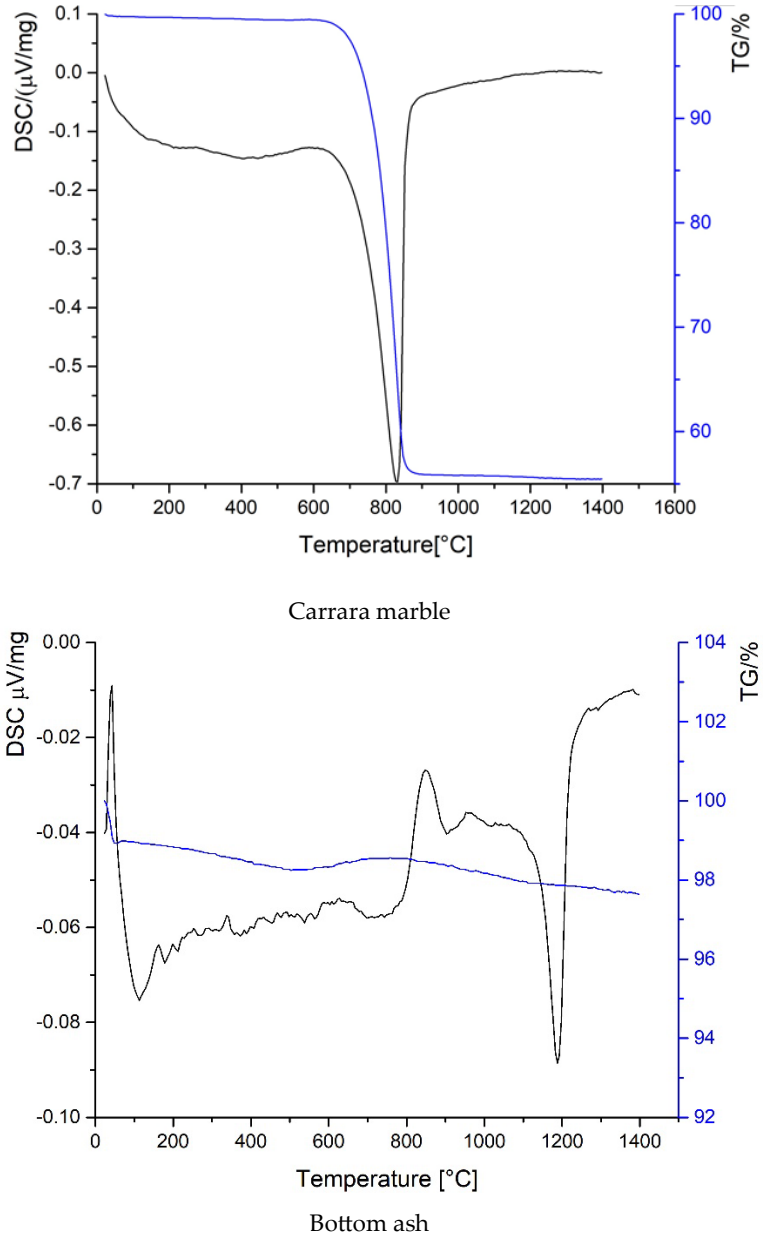

Figure 7. Thermogravimetric and differential thermal analysis (TG/DSC) bottom ash and Carrara marble.

Table 6. Particle Size Analysis of SRM (D10-D50-D90).

	D10 (μm)	D50 (μm)	D90 (μm)
Carrara Marble	1.886	9.479	30.473
Bottom Ash	38.903	192.521	560.032
Foundry Sand	57.972	100.219	164.317

3.3. Characterization of New Formulations

Post-firing characterization of the samples produced from the newly developed ceramic bodies was performed by measuring linear shrinkage, water absorption, and apparent density. Additional microstructural and compositional investigations were carried out using scanning electron microscopy (SEM) coupled with energy-dispersive X-ray spectroscopy (EDS), as well as X-ray diffraction (XRD) to assess phase composition. The linear shrinkage (LS, %) values of all fired samples are reported in Table 7. All measured values were $\leq$1%, with the exception of the formulations containing bottom ash, which exhibited comparatively higher shrinkage. The parameter ΔS represents the difference between the shrinkage of each tested sample and that of the standard formulation. The water absorption (WA, %) values are also reported in Table 7. The parameter ΔA represents the difference between the water absorption of each tested sample and that of the standard formulation.

Table 7. The linear shrinkage (%) and water absorption (%) results for post-firing samples with the respective ΔS and ΔA differences from the standard values.

Sample	% SRM	Shrinkage % (±0.1)	Water Absorption % (±0.01)	ΔA	ΔS
FS 10	10	1	16.28	−0.84	0.7
FS 50	50	0.8	16.97	−0.15	0.5
FS 100	100	0.8	16.39	−0.73	0.5
CM 10	10	0.3	16.66	−0.46	0
CM 50	50	−0.1	17.68	0.56	−0.4
CM 100	100	−0.1	17.33	0.21	−0.4
BA10	10	1.2	18.07	0.95	0.9
BA 50	50	4.1	12.79	−4.33	3.8
BA 100	100	9.3	0.53	−0.59	9
Standard	/	0.3	17.12	/	/

At typical monoporosa firing temperatures, bottom ash exhibits high fusibility; therefore, when added in significant amounts, it markedly accelerates the vitrification process. By comparing the chemical analysis of bottom ash with that of STD sand, it is observed that the ash contains higher percentages of magnesium, potassium, and iron oxides. The presence of these oxides in the ash influences the sintering process of the sample by reducing viscosity and increasing shrinkage, as described by the Frenkel model [34]. Indeed, when sand is completely replaced by bottom ash, the resulting linear shrinkage increases significantly. Correspondingly, water absorption decreases to 0%, indicating complete densification of the ceramic body. These results demonstrate that bottom ash is not suitable as a replacement for sand in monoporosa formulations, as it leads to excessive sintering. Conversely, owing to its high reactivity at elevated temperatures, bottom ash appears more suitable for use in porcelain stoneware bodies, which require higher firing temperatures to achieve proper sintering. Among all the secondary raw materials (SRMs) investigated, foundry sand emerges as the most promising candidate. At 1156 °C, linear shrinkage values range between 0% and 1%, indicating good dimensional stability. Unlike sludge-based materials, which tend to act as binders and increase slip viscosity after milling, foundry sand does not adversely affect the rheological properties of the suspension.

A complete (100%) replacement of calcite also results in a favorable shrinkage behavior, with a reference shrinkage value of −0.10% at 1156 °C, as reported in Table 7. Based on these results, the most promising secondary raw materials were identified. Foundry sand was selected as a substitute for conventional sand. Carrara marble sludge was identified as a replacement for calcite.

Table 8 reports the crystalline phases identified in samples containing the highest contents of secondary raw materials (50% and 100%). Samples incorporating 50% and 100% Carrara marble do not exhibit significant mineralogical differences, with quartz and calcic albite identified as the main crystalline phases. Similarly, in samples containing foundry sand, no substantial differences are observed between the two substitution levels. Quartz and albite remain the predominant crystalline phases detected.

Table 8. Crystalline phases from XRD analysis of formulations with 50% and 100% of sand and sludge.

Sample	Crystalline Phase	Ref. Code
FS 50	- Quartz - Albite calcian low	- 01-083-0539 - 01-076-0927
FS 100	- Quartz - Albite calcian low	- 01-083-0539 - 01-076-0927
CM 50	- Quartz - Albite calcian, ordered	- 01-083-0539 - 00-041-1480
CM 100	- Quartz - Albite calcian, ordered	- 01-083-0539 - 00-041-1480

Figure 8 presents field-emission gun scanning electron microscopy (FEG-SEM) micrographs of sample CM100, containing 100% Carrara marble sludge, acquired at magnifications of 1600× and 6000×. The ceramic matrix exhibits a porous microstructure, with pores appearing to be uniformly distributed throughout the body. Energy-dispersive X-ray spectroscopy (EDS) analysis confirms the presence of Ca-rich regions surrounding the pores, as observed in Area 2, while the matrix (Area 1) is mainly composed of Si-, Al-, and Ca-bearing oxides. In the FS100 sample, composed of 100% foundry sand, bright particles are observed in localized regions of the matrix. EDS analysis of these areas reveals the presence of silicon (Si), zirconium (Zr), aluminum (Al), and calcium (Ca), indicating that these particles correspond to the crystalline phases identified by XRD analysis. The carbon detected in the EDS spectra of both samples is attributed to surface contamination introduced during sample preparation.

Subsequently, a colorimetric evaluation was performed for each formulation. The variations in the CIE Lab* parameters with respect to the standard composition are reported in Table 9. Changes in the percentage of secondary raw material used to replace the conventional raw material result in variations in the ΔE values, which may or may not be significant depending on the intended application of the ceramic body. In general, ΔE values lower than 1 are considered imperceptible, while values between 1 and 2 are regarded as barely perceptible. However, the acceptable industrial range of ΔE is typically between approximately 2.5 and 3. In the case of Carrara marble sludge used as a substitute for calcite, only minor variations in the colorimetric parameters were observed. These variations increased slightly with replacement levels. The measured values remained very close to those of the standard sample. In contrast, the use of foundry sand led to more pronounced color variations. This effect is due to its intrinsic coloration associated with iron content, which affected the L, a, and b parameters. As result, higher ΔE values were observed compared with samples containing Carrara marble sludge. Nevertheless,

this does not represent a critical issue, as these ceramic bodies are intended as support substrates and can be subsequently coated with a glaze.

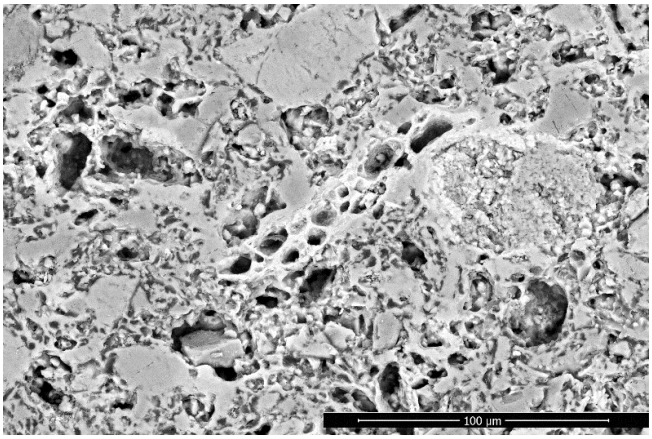

(**a**) 1600×

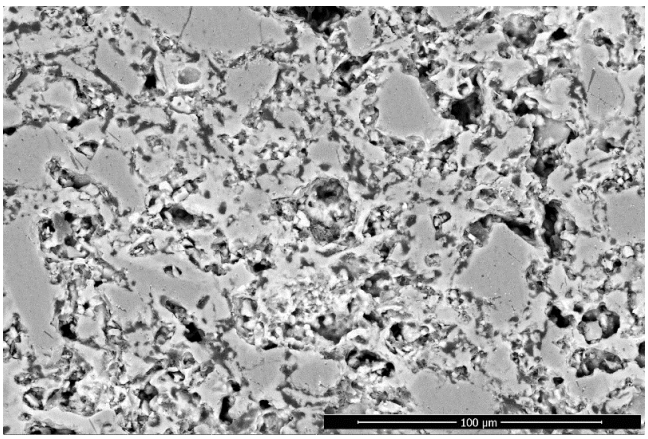

(**b**) 1600×

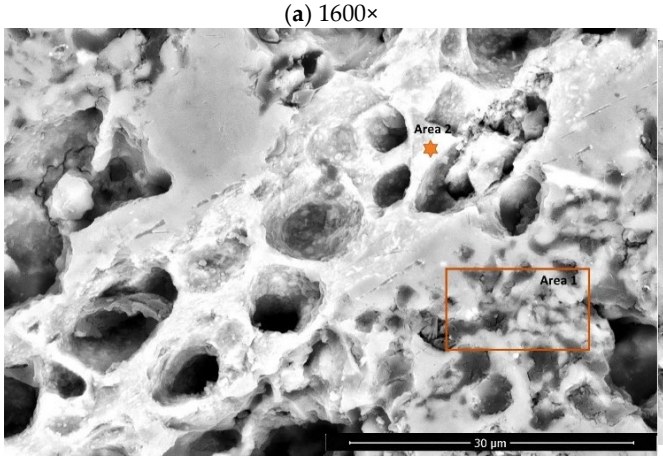

(**c**) 6000×

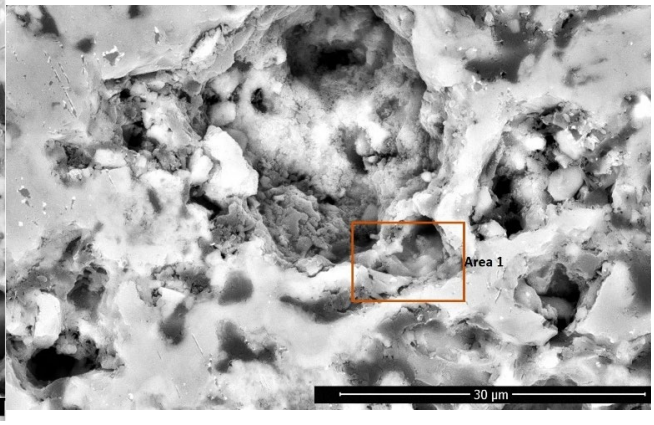

(**d**) 6000×

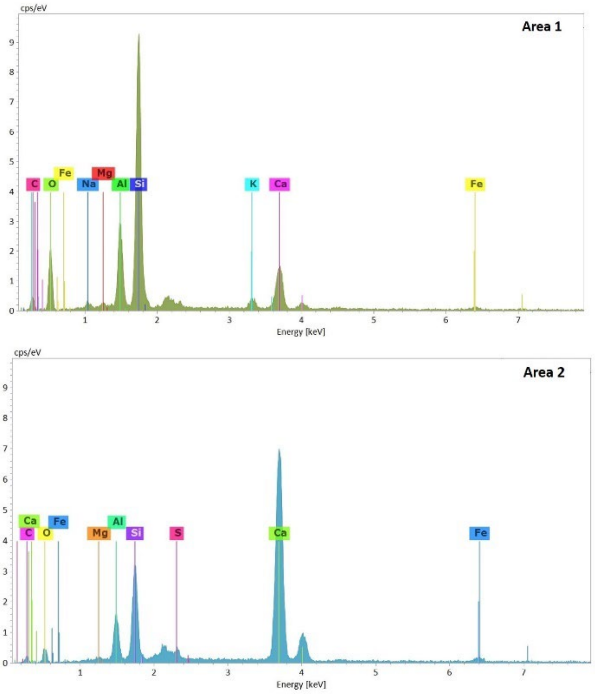

(**e**) EDS analysis Area 1–Area 2
CM 100

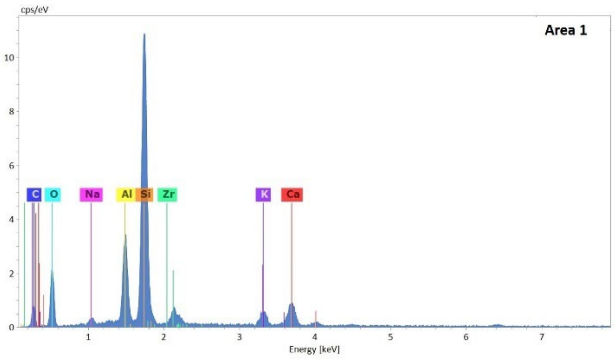

(**f**) EDS analysis Area 1
FS 100

Figure 8. SEM and EDS analysis of best samples with 100% of sand (FS100) and sludge (CM100).

Table 9. Labparameters with respect to the standard composition of samples.

Sample	L*	a*	b*	ΔE
STD	76.9	4.84	14.53	/
CM 100	77.45	5.12	16.16	1.74
FS 100	76.13	3.15	11.41	3.63

The thermal expansion coefficient (α) of the two most promising formulations was also evaluated and compared with the standard body. The results (Table 10), obtained in the temperature range of 200–400 °C, show a slight increase in α for the two new formulations. However, the values remain within acceptable limits for single-firing (monoporosa) ceramic bodies.

Table 10. Thermal expansion coefficient of samples with 100% foundry sand and 100% Carrara marble.

Sample	α (°C^{-1}) ($\pm$0.001)
STD	7.339×10^{-6}
CM 100	5.964×10^{-6}
FS 100	5.931×10^{-6}

4. Conclusions

This study aimed to develop more sustainable single-fired (monoporosa) ceramic bodies by partially replacing traditional raw materials with secondary raw materials (SRMs) derived from industrial processes. A standard reference body and the most promising low-impact formulations were characterized in terms of their chemical, mineralogical, and morphological properties. Technological properties, including linear shrinkage, apparent density, and water absorption, were evaluated for all developed bodies. The selected SRMs were characterized and classified according to their compatibility with monoporosa formulations. In addition, the influence of SRM substitution on water absorption behavior was investigated, together with a preliminary assessment of its effect on the thermal expansion coefficient. Based on the obtained results, particularly those related to shrinkage and water absorption performance, two formulations emerged as the most similar to the standard body and the most suitable for potential industrial-scale trials. Specifically, the CM100 and FS100 formulations exhibited linear shrinkage values of -0.1% and 0.8%, respectively, i.e., below 1% and within industrial tolerance limits, as well as water absorption values of 16–17%, which are fully comparable to that of the standard formulation (17%). Furthermore, from a morphological and microstructural standpoint, no significant differences affecting the overall performance were observed, even when 100% substitution with SRMs was applied. Colorimetric analysis also indicated that the ΔE values fall within the acceptable industrial range of 2.5–3. Therefore, it can be concluded that the two investigated secondary raw materials—namely Carrara marble and foundry sand—are well suited for use in monoporosa ceramic bodies and can contribute to the development of more sustainable and circular construction materials. Indeed, excluding the clay component (44 wt.% of the formulation), a monoporosa body containing up to 56 wt.% recycled materials can be achieved. Further improvements may be explored in future studies to enhance industrial performance, for example, by increasing the thermal expansion coefficient, which at an industrial level would broaden the range of compatible glazes that can be applied on the surface. In addition, regarding foundry sand, industrial-scale application would require careful monitoring of supply homogeneity, particularly with respect to iron content. Iron oxides, acting as fluxing agents, may significantly alter the sintering process above certain

threshold concentrations, thereby affecting all the key technological parameters of the ceramic body, including firing behavior, shrinkage, and dimensional stability. Moreover, attention should be paid to stress-relief (annealing) phenomena typically observed in large-format monoporosa products.

Author Contributions: C.S. (Caterina Sgarlata): Investigation, Data curation, Writing—original draft, Writing—review and editing, Visualization. L.C.: Visualization, Writing—review and editing. L.S.: Validation, Formal analysis, Investigation, Resources. C.S. (Cristina Siligardi): Conceptualization, Methodology, Validation, Formal Analysis, Resources, Data curation, Writing—review and editing, Visualization, Supervision, Project administration. All authors have read and agreed to the published version of the manuscript.

Funding: This research was funded by Ministero delle imprese e del made in Italy: Prog. n° F/310058/01/X56.

Data Availability Statement: The original contributions presented in this study are included in the article. Further inquiries can be directed to the corresponding authors.

Acknowledgments: The authors wish to extend their gratitude to all the industry and academic collaborators and experts, Francesca Terzi, Lincy Varghese, Paola Miselli, Miriam Hanuskova, Mariangela Governatori of UNIMORE and for their indispensable and timely support in facilitating the completion of this investigation.

Conflicts of Interest: Lorenzo Serafini was employed by Gruppo Concorde S.p.A. The authors declare that they have no known competing financial interests or personal relationships that could have appeared to influence the work reported in this paper.

References

1. Sánchez, E.; García-Ten, J.; Sanz, V.; Moreno, A. Porcelain tile: Almost 30 years of steady scientific-technological evolution. *Ceram. Int.* **2010**, *36*, 831–845. [CrossRef]
2. Lasić, J.; Šimunović, K. Ceramics as an important element of design and architecture. *E-Zb. Electron. Collect. Pap. Fac. Civ. Eng.* **2025**, *15*, 84–106. [CrossRef]
3. Mourou, C.; Zamorano, M.; Ruiz, D.P.; Martín-Morales, M. Characterization of ceramic tiles coated with recycled waste glass particles to be used for cool roof applications. *Constr. Build. Mater.* **2023**, *398*, 132489. [CrossRef]
4. Amin, S.H.K.; Elmahgary, M.G.; Abadir, M.F. Preparation and characterization of dry pressed ceramic tiles incorporating ceramic sludge waste. *Ceram.-Silik.* **2019**, *63*, 11–20. [CrossRef]
5. Brasileiro, C.T.; Conte, S.; Contartesi, F.; Melchiades, F.G.; Zanelli, C.; Dondi, M.; Boschi, A.O. Effect of strong mineral fluxes on sintering of porcelain stoneware tiles. *J. Eur. Ceram. Soc.* **2021**, *41*, 5755–5767. [CrossRef]
6. Siligardi, T.C.; Manfredini, D.; Settebre Blundo, M.; Montosi, P.M. Analisi Microstrutturale E Tecnologica Di Impasti Da Monoporosa Di Produzione Industriale I Parte. *Ceram. Inf. Ed.* **2003**, *424*, 347–353–.
7. Barrachina, E.; Esquinas, M.; Llop, J.; Notari, M.D.; Carda, J.B. Development of a glass-ceramic glaze formulated from industrial residues to improve the mechanical properties of the porcelain stoneware tiles. *Mater. Lett.* **2018**, *220*, 226–228. [CrossRef]
8. Cheever, E. *Kitchen & Bath Products and Materials: Cabinetry, Equipment, Surfaces*; John Wiley & Sons: Hoboken, NJ, USA, 2014.
9. Raimondo, M.; Dondi, M.; Zanelli, C.; Guarini, G.; Gozzi, A.; Marani, F.; Fossa, L. Processing and properties of large-sized ceramic slabs. *Bol. De La Soc. Esp. De Cerám. Y Vidr.* **2010**, *49*, 289–296.
10. Bertoni, M.A.; Reginelli, A.; Rovini, D.; Settembre, C.; Siligardi, C.; Lugli, M.M. Reattività di alcuni carbonati con illite e caolinite negli impasti da monoporosa. *Ceram. Inf.* **2007**, *69*, 110–120.
11. Kayaci, K. Effect of fluxing raw materials on moisture expansion of monoporosa wall tile bodies. *J. Therm. Anal. Calorim.* **2021**, *146*, 1603–1611. [CrossRef]
12. Ustunel, G.; Yenikaya, C.; Bekmezci, M.; Sen, F. Prevention of mat glazed acid permeability used in monoporosa wall ceramics. *Environ. Technol. Innov.* **2021**, *23*, 101628. [CrossRef]
13. Siligardi, C.; Settembre, D.; Montorsi, M.; Reginelli, M. Reactivities of carbonates with illite and kaolinite in monoporosa wall tiles. In Proceedings of the 2nd International Congress on Ceramics, ICC 2008, Verona, Italy, 29 June–4 July 2008; pp. 1–7.
14. Soares, L.; Dal-Bó, A.G.; Bernardin, A.M. Use of enameling wastewater in the wet milling process for 'monoporosa' tile composition. *Clean. Eng. Technol.* **2021**, *5*, 100338. [CrossRef]

15. Dondi, M. Technological and compositional requirements of clay materials. In *A Clay Odyssey*; Domínguez, E.A., Mas, G.R., Cravero, F., Eds.; Elsevier: Amsterdam, The Netherlands, 2001; Volume 1, pp. 23–30.
16. Reginelli, D.M.; Settembre, A.; Bertoni, A.; Rovini, M.G.; Vezzalini, A.; Gualtieri, G.C. Ottimizzazione di impasti da monoporosa. *Ceram. Inf.* **2004**, *438*, 855–868.
17. Gualtieri, A.F. Thermal behavior of the raw materials forming porcelain stoneware mixtures by combined optical and *In Situ* X-ray dilatometry. *J. Am. Ceram. Soc.* **2007**, *90*, 1222–1231. [CrossRef]
18. Savvova, O.; Pokroieva, Y.; Luhovoi, I.; Smyrnova, Y.; Pylypenko, O. Using of wastes from the enrichment of quartz-feldspar raw materials in the production of porcelain stoneware. *IOP Conf. Ser. Earth Environ. Sci.* **2024**, *1376*, 012025. [CrossRef]
19. López-Perales, J.F.; Sánchez-Rodríguez, R.; Suárez-Suárez, D.D.; Rodríguez, E.A. Fired electrical porcelain scrap (chamotte waste) recycling and reuse as an alternative raw material for sustainable porcelain stoneware production. *J. Clean. Prod.* **2024**, *434*, 140385. [CrossRef]
20. Torres, P.; Manjate, R.S.; Quaresma, S.; Fernandes, H.R.; Ferreira, J.M.F. Development of ceramic floor tile compositions based on quartzite and granite sludges. *J. Eur. Ceram. Soc.* **2007**, *27*, 4649–4655. [CrossRef]
21. Silvestri, L.; Forcina, A.; Silvestri, C.; Falcone, D. Life Cycle Assessment of circular economy strategies for the eco-design of ceramic bricks incorporating olive and wine residues: Advancing sustainability through agro-industrial byproducts. *Sci. Total Environ.* **2026**, *1011*, 181153. [CrossRef]
22. Rotilio, M.; Cucchiella, F.; Annibaldi, V. Secondary Raw Materials for Circular Economy in Construction Sector: A Review. *Key Eng. Mater.* **2022**, *919*, 260–269. [CrossRef]
23. Khater, G.A.; Romero, M.; López-Delgado, A.; Padilla, I.; El-Kheshen, A.A.; Farag, M.M.; Elmaghraby, M.S.; Nasralla, N.H.S.; Shendy, H. Novel ceramic materials based on industrial wastes within the CaO–MgO–Al_2O_3–SiO_2 system. *Mater. Chem. Phys.* **2025**, *331*, 130178. [CrossRef]
24. Sgarlata, C.; Formia, A.; Ferrari, F.; Piccolo, F.; Leonelli, C. Metakaolin addition to improve geopolymerization process and properties of waste clay-based materials. *Solid State Phenom.* **2021**, *325*, 137–142. [CrossRef]
25. Khan, A.A.; de Jong, W.; Jansens, P.J.; Spliethoff, H. Biomass combustion in fluidized bed boilers: Potential problems and remedies. *Fuel Process. Technol.* **2009**, *90*, 21–50. [CrossRef]
26. James, A.K.; Thring, R.W.; Helle, S.; Ghuman, H.S. Ash Management Review—Applications of Biomass Bottom Ash. *Energies* **2012**, *5*, 3856–3873. [CrossRef]
27. Monteleone, B.; Baldereschi, E.; Fabbri, N.; De Bernardi, C.; Frey, M. A sustainability assessment of the foundry production process in Italy. *Sustain. Prod. Consum.* **2024**, *46*, 491–501. [CrossRef]
28. Sgarlata, C.; Ariza-Tarazona, M.C.; Paradisi, E.; Siligardi, C.; Lancellotti, I. Use of Foundry Sands in the Production of Ceramic and Geopolymers for Sustainable Construction Materials. *Appl. Sci.* **2023**, *13*, 5166. [CrossRef]
29. Bhardwaj, A.; Kumar, P.; Siddique, S.; Shukla, A. Comprehensive review on utilization of waste foundry sand in concrete. *Eur. J. Environ. Civ. Eng.* **2023**, *27*, 1056–1087. [CrossRef]
30. Xiang, R.; Li, Y.; Li, S.; Xue, Z.; He, Z.; Ouyang, S.; Xu, N. The potential usage of waste foundry sand from investment casting in refractory industry. *J. Clean. Prod.* **2019**, *211*, 1322–1327. [CrossRef]
31. Tazzini, A.; Gambino, F.; Casale, M.; Dino, G.A. Managing Marble Quarry Waste: Opportunities and Challenges for Circular Economy Implementation. *Sustainability* **2024**, *16*, 3056. [CrossRef]
32. Eurostat Statistic Explained Waste Statistics. 2023. Available online: https://ec.europa.eu/eurostat/statistics-explained/index.php?title=Waste_statistics (accessed on 2 April 2024).
33. Gómez-Tena, M.P.; Gilabert, J.; Zumaquero, E.; Díaz-Canales, E.M.; Arrufat, S.; Domínguez, R. Reactivity of crystalline silica in processing ceramic tiles. *Qualicer* **2024**, 1–14.
34. Frenkel, J.A. Viscous flow of crystalline bodies under the action of surface tension. *J. Phys. USSR* **1945**, *9*, 385–391.